DOI: 10.1002/maco.201408112

Prediction of the long-term corrosion rate of copper alloy objects

K. Kreislova* and H. Geiplova

Comparative atmospheric corrosion data for different metal alloys can be used to predict the service life of a component, maintenance requirements, and metal loss to the environment. In some international projects some prediction models have been derived for the atmospheric corrosion rate of metals – dose/response functions (EN ISO 9224, ECE UN ICP program, Multi-Assess project) – including copper alloys.

In this paper, actual corrosion studies of two long-term exposed objects – a bronze statue of John of Nepomuk from Charles Bridge and the copper roof of Queen Ann's Summer Palace, are presented. Both these objects are exposed to Prague's urban atmosphere for more than 300 years. The predicted and measured corrosion rates are compared for these cultural objects. During their exposure the corrosion rates changed as the result of changing corrosivity of atmosphere in the Prague centre.

1 Introduction

Historically, objects made from copper/copper alloy were used for religious and artistic objects. The properties of copper and their alloys make them suitable for use as outdoor architectural objects. Different studies related to copper alloy heritage objects from point of view of patina detailed analysis, restoration and conservation, but there is a lack of studies focused onto their long-term corrosion behaviour in outdoor atmospheric environments.

Due to the many suitable properties of copper, it was used as the roofing material of many buildings since ancient times. Many important historic buildings are covered by sheet copper roofs - castles, cathedrals, churches, palaces, etc. Historic roofing reflects the availability of materials, the levels of construction technology and the environmental conditions.

Bronze was used for the construction of different types of works of art, statues and monuments of cultural relevance due to its high stability regarding atmospheric corrosion. The corrosion of bronze monuments was studied in many projects. This interest is mainly due to the increased awareness of air pollution damage to cultural heritage. Some works have contributed to a better understanding of the reaction mechanisms of environmental deterioration.

In atmospheric environments, metallic materials are damaged by basic climatic factors such as temperature and relative humidity. Metal corrosion occurs on the surface layer of the electrolyte – the phase of moisture film. One significant factor affecting the atmospheric corrosion of metals is wetness duration (time of wetness TOW), i.e., the period during which an electrolyte film exists on the metal surface. In Europe, TOW is ca 4000 hrs.a^{-1} for the majority of the territory.

Corrosion stress is increased by air pollution – gaseous and/or solid, which is able to dissolve and ionise in the moisture film. The complex effect of atmospheric environments on atmospheric corrosion is very difficult to quantify due to the variability of its parameters. The decisive effect of sulphur dioxide (SO_2) on metal corrosion was shown in many field exposures [1–3], so for the corrosivity of the atmosphere, the most significant factor was the increasing concentration of air pollution featuring sulphur dioxide or SO_2. Its concentration increased relatively slowly during the 18th century but rose dramatically after 1945. In Europe, a great reduction in main air anthropogenic emissions has occurred over the last 25 years; SO_2 levels declined significantly since 1990s, which has resulted in a decrease in atmospheric corrosivity as well. The trends of changes in atmospheric corrosivity and the long-term corrosion rate of structural metals were systematically evaluated in many studies [4]. These studies have been used for the revision of ISO standards for atmospheric corrosivity classification.

2 Corrosion behaviour of copper alloy

Copper is a relatively active metal which, when left unprotected, tends to oxidize/corrode. Long-term atmospheric exposure generally results in the formation of a naturally protective patina which colour changes starting from a dull brown to black spots – cuprite, and finally to green – antlerite and/or brochantite (or greenish-blue in marine localities - atacamite). The colour is

K. Kreislova
SVUOM Ltd., U Mestanskeho pivovaru 934, Prague 170 00, (Czech Republic)
E-mail: kreislova@svuom.cz

H. Geiplova
UTAM/CET, Batelovská 485, 486 588 56, Telč, (Czech Republic)

controlled by the amount of patina and its chemical composition. Over the centuries, this patina is thought to provide an aesthetically pleasing appearance to copper roofs. If the patina is sufficiently thick – minimally 15 μm in total, it is green.

Its colour indicates that the copper has been around for a long period of time as it takes many years to form a thick green patina [4–6]. Cuprite layer grows with rate 0.2 to 2.0 μm.a^{-1} till steady state with thickness 5–10 μm. Green corrosion products form with rate ca 0.15 μm.a^{-1}. However, the corrosion loss of copper or bronze cannot be estimated according the colour or composition of the patina layer as it is reactive to many factors related to atmospheric environment.

The corrosion behaviour of bronze in atmospheric environments was not studied as thoroughly as copper, but some data are available. Patina forms slowly and slightly differs according to the bronze composition – trace compounds of alloying elements may be found (e.g. lead, tin) especially in the initial period of exposure. During long-term exposure the bronze composition affects the colour of the patina more than corrosion mass loss. Atmospheric corrosion mass loss of bronze is usually two-thirds the corrosion mass loss of copper, as was verified by field exposure programmes.

Corrosion mass loss by uniform metal corrosion can be estimated according to EN ISO 9223 [7] and EN ISO 9224 [8] or other dose-response functions derived in the research projects Multi-Assess, UN ECE ICP Materials, etc. Copper alloys (copper, bronze) were exposed in all of these exposure projects in a large set of atmospheric test sites, e.g.:

-ISOCORRAG exposure programme - 53 test sites in 13 countries on four continents, copper,

$$\begin{aligned}\text{copper}\quad r_{corr} &= 0.0053[SO_2]^{0.26}\exp(0.059RH + f(T)) \\ &\quad + 0.0125[Cl^-]^{0.27}\exp(0.036RH + 0.049T) \\ f(T)Cu &= 0.126(T-10)\ \text{when}\ T \leq 10\,^{\circ}C, \\ &\quad \text{otherwise} - 0.080(T-10)\end{aligned} \tag{1a}$$

$$\text{bronze}\quad r_{corr} = \frac{2}{3}\, r_{corr}(Cu) \tag{1b}$$

MICAT exposure programme - 72 test sites in 14 Ibero-American countries, copper,

Multi-Assess project - 28 test sites in 16 countries in Europe, copper and bronze (6–8 wt% Sn, 3–5 wt% Zn, 5–7 wt% Pb),

$$\begin{aligned}\text{copper}\quad ML_1 &= 3.12 + \left\{1.09 + 0.00201[SO_2]^{0.4}[O_3]RH \cdot e^{f(T)} \right. \\ &\quad \left. + 0.0878Rain[H^+]\right\}t \\ f(T) &= 0.083(T-10)\ \text{when}\ T < 10\,^{\circ}C, \\ &\quad \text{otherwise} - 0.032(T-10)\end{aligned} \tag{2a}$$

$$\begin{aligned}\text{bronze}\quad ML_1 &= 1.33 + \left\{0.00876[SO_2]RH \cdot e^{f(T)} \right. \\ &\quad \left. + 0.0409Rain[H^+] + 0.0380PM_{10}\right\}t \\ f(T) &= 0.060(T-11)\ \text{when}\ T < 11\,^{\circ}C, \\ &\quad \text{otherwise} - 0.067(T-11)\end{aligned} \tag{2b}$$

UN ECE ICP exposure programme – 39 test sites in 12 countries in Europe, USA and Canada, copper and bronze (6 – 8 wt% Sn, 3 – 5 wt% Zn, 5 – 7 wt% Pb) [9]

$$\begin{aligned}\text{copper}\quad ML_2 &= 0.0027[SO_2]^{0.32}[O_3]^{0.79}RH \cdot e^{f(T)}t^{0.78} \\ &\quad + 0.050Rain[H^+]t^{0.89} \\ f(T) &= 0.083(T-10)\ \text{when}\ T < 10\,^{\circ}C, \\ &\quad \text{otherwise} - 0.032(T-10)\end{aligned} \tag{3a}$$

$$\begin{aligned}\text{bronze}\quad ML_2 &= 0.026[SO_2]^{0.44}RH \cdot e^{f(T)}t^{0.86} \\ &\quad + (0.029Rain[H^+] + 0.00043Rain[Cl^-])t^{0.7} \\ f(T) &= 0.060(T-11)\ \text{when}\ T < 11\,^{\circ}C, \\ &\quad \text{otherwise} - 0.067(T-11)\end{aligned} \tag{3c}$$

The symbols used in equations are:

- r_{corr} - first year corrosion rate of metal in μm.a^{-1},
- ML – total corrosion mass loss after exposure in g.m^{-2} or total corrosion loss after exposure in μm,
- t – time of exposure in years (a),
- T – yearly average temperature in °C,

Note: As the corrosion rate depends on temperature, this parameter T is used in equations in different format f(T) written below the equation according to yearly average temperature in locality.

- RH – yearly average relative humidity in %,
- $[SO_2]$ – yearly average sulphur dioxide deposition rate in mg.m^{-2}.day^{-1} in ISO 9223 standard equation and yearly average sulphur dioxide concentration in mg.m^{-3} in the other equations,
- $[Cl^-]$ – yearly average chloride deposition rate in mg.m^{-2}.day^{-1} in ISO 9223 standard equation and yearly average precipitation concentration in mg.l^{-1} in the other equations,
- $[O_3]$ – yearly average ozone concentration in air (air pollution) in μg.m^{-3},
- PM_{10} – yearly average concentration of particle matter with dimension lower than 10 μm in air (air pollution) in μg.m^{-3},
- Rain – yearly sum of precipitation in mm,
- $[H^+]$ – yearly average hydrogen ion concentration in precipitation in mg.l^{-1}.

Comparisons of determined and predicted yearly corrosion mass loss of copper are given in Figure 1. All prediction models included some uncertainty for dose-response functions – the best fitting values for copper corrosion in the period 2011-12 within the framework of the UN ECE ICP *Effect on Material* programme was estimated for the ISO equation. All prediction models were derived from database obtaining mainly the corrosion and environmental data from period when the SO_2 was more dominant factor of the atmospheric corrosion. The R^2 values are relative low for actual data. The comparison of

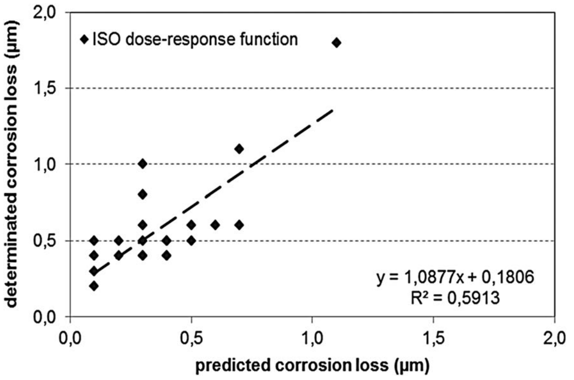

Figure 1. Comparison of determined and predicted corrosion mass loss of copper.

Table 1. Guiding corrosion values for corrosion rates (r_{av}, r_{lin}) of copper in atmospheres of classified corrosivity categories (μm.a^{-1})

C1	C2	C3	C4	C5	CX
Average corrosion rate (r_{av}) during the first 10 years					
$r_{av} \leq 0.05$	$0.05 < r_{av} \leq 0.3$	$0.3 < r_{av} \leq 0.6$	$0.6 < r_{av} \leq 1.3$	$1.3 < r_{av} \leq 2.6$	$2.6 < r_{av} \leq 4.6$
Steady state corrosion rate (r_{lin}) estimated as the average corrosion rate during the first 30 years					
$r_{lin} \leq 0.03$	$0.03 < r_{lin} \leq 0.2$	$0.2 < r_{lin} \leq 0.4$	$0.4 < r_{lin} \leq 0.9$	$0.9 < r_{lin} \leq 1.8$	$1.8 < r_{lin} \leq 3.2$

prediction models for bronze alloy is very similar, but the R^2 value is higher.

For some dose-response models, the long-term equation was derived and *t* (time) was one of the equation parameters so they could be used for long-term corrosion loss predictions. The kinetic model of long-term exposure was used for atmospheric corrosion in the ISO 9224 standard including r_{corr} and the time parameter:

$$ML_3 = r_{corr} t^b \tag{4}$$

More general guiding corrosion values given in intervals of average corrosion rates for corrosivity categories may be preferred (EN ISO 9224 Annex B). Average corrosion rates up to 10 years are considered to correspond to the initial period of exposure - see Table 1. Average corrosion rates for periods longer than 10 years are considered to be steady state corrosion rates.

The corrosion mass losses of copper and bronze in sheltered locations protected against direct precipitation are lower than those estimated in open atmospheres (Figure 2). There are many such surfaces on actual objects/statues.

For bronze alloys, the corrosion rate depends on the alloy composition. Within the framework of the EUREKA project E!2210 *Bronzart Artistic bronze: Selection of alloys, protective evaluation using conventional and advanced techniques,* bronze samples with different compositions were exposed at atmospheric test sites (Table 2). After 1 year of exposure, the red-brown surface of bronze alloys containing lead and zinc (No. 1, No. 7) was covered by white and green spots of the corrosion product of these elements and copper. After 10 years of exposure the dark surface is covered by green spots of the corrosion products. The total corrosion mass losses ranged from 4.5 to 6.5 μm with a corrosion rate of ca. 0.6 μm.a^{-1}. The actual yearly corrosion loss of copper at this locality is 1.7 μm, so the corrosion loss of bronze is one-third that of the corrosion mass loss of copper. The differences in corrosion rates of different bronze alloys are not significant.

Patinas are heterogeneous and metallurgical complexes that come in a variety of colours. The colour is determined by the "age" and thickness of the patina and its chemical composition.

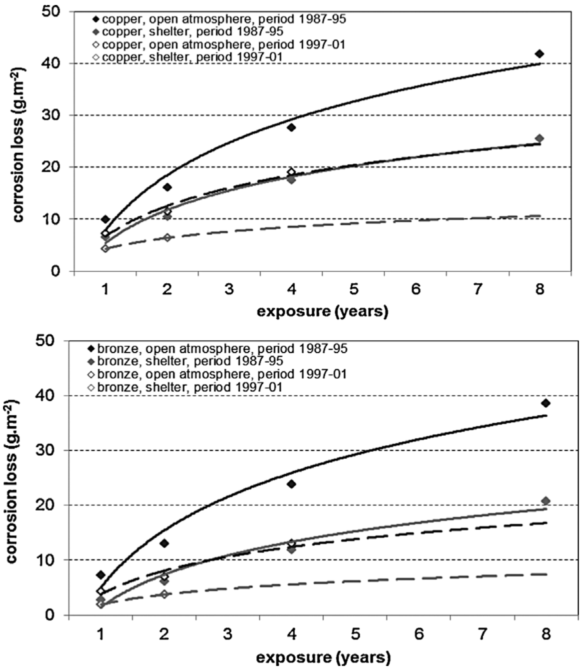

Figure 2. Corrosion mass loss of copper and bronze in open and sheltered atmospheric exposure.

Table 2. Chemical composition of tested bronze samples

bronze alloy	composition (wt. %)								
	Cu	Sn	Pb	Zn	Si	Ni	Fe	Mn	Bi
No. 1	85.00	5.00	5.00	5.00					
No. 5	89.00	8.00			3.00				
No. 6	87.24	9.50				3.16	0.06	0.04	
No. 7	86.33	7.76	3.00		2.91				
No. 8	86.33	7.76			2.91				3.00

Green patinas are typically characterised by an outer layer of antlerite and/or brochantite, which forms as individual crystals on the surface of the cuprite layer. The thickness of the outer layer varies from 10 to 84 μm, but on average does not exceed 45–50 μm. The patina's colour seems green after reaching the homogenous layer of antlerite or brochantite with thickness ca. 5 μm, i.e., total thickness of the patina layer min. 15 μm.

The thickness of the patina layers was measured and an analysis of the patina was carried out in some field exposure programmes. The thickness of the patina layers on bronze samples exposed for 10 years (*Bronzart* project) varied from 6 to 20 μm and a non-uniform green layer occurred on the sampleś surfaces.

3 Change in atmospheric corrosion mass loss

The effect of changes in atmospheric corrosivity in urban localities can be illustrated using the results of the UN ECE ICP programme, where the standard copper and bronze samples were exposed over different periods [9–10]:

1987-1995–copper and bronze for 1, 2, 4 and 8 years,
1997-2001–copper and bronze for 1, 2 and 4 years,
2011-2012–copper for 1 year.

A comparison of yearly copper mass loss at the European test sites in these periods is given in Figure 3. The trend of decreasing yearly copper corrosion mass loss is not as significant as in the other metals (carbon steel, zinc).

At atmospheric test sites in the Czech Republic the standard copper and bronze samples were exposed as part of national and other international projects. The dependence of the decreasing rate of mass loss of copper on SO_2 air pollution (steady pollution situation) is illustrated in Figure 4. The actual corrosion rate of

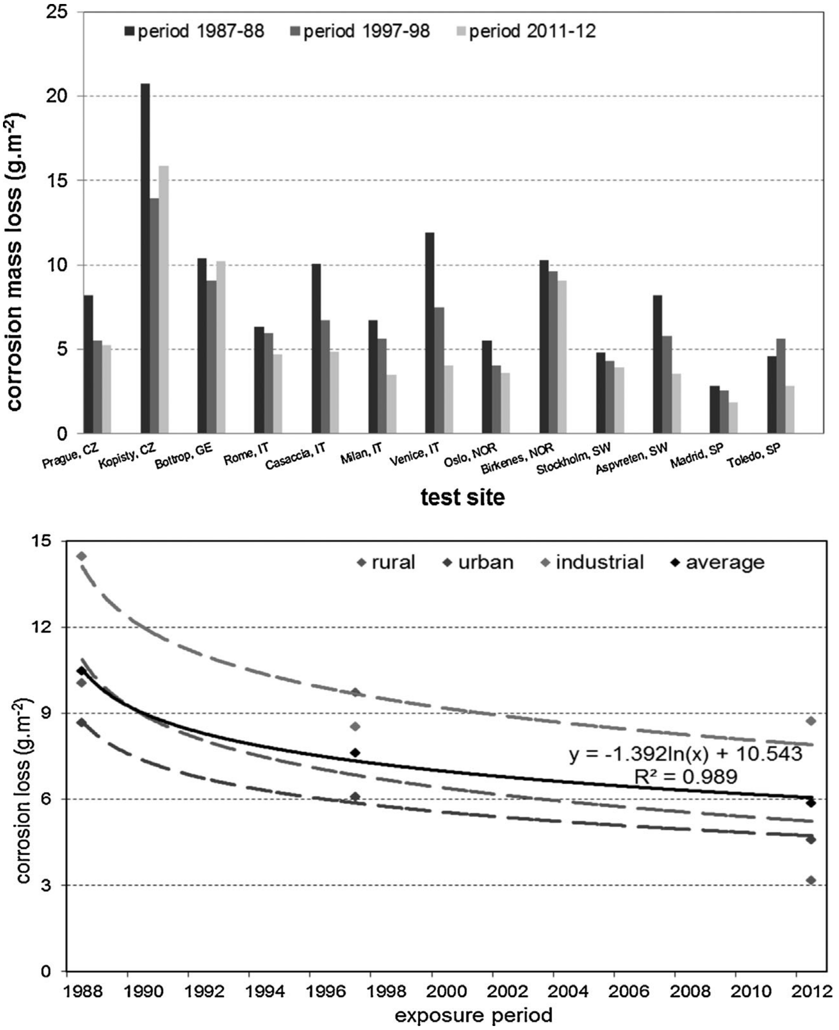

Figure 3. Change in corrosion mass loss of copper over various periods in Europe.

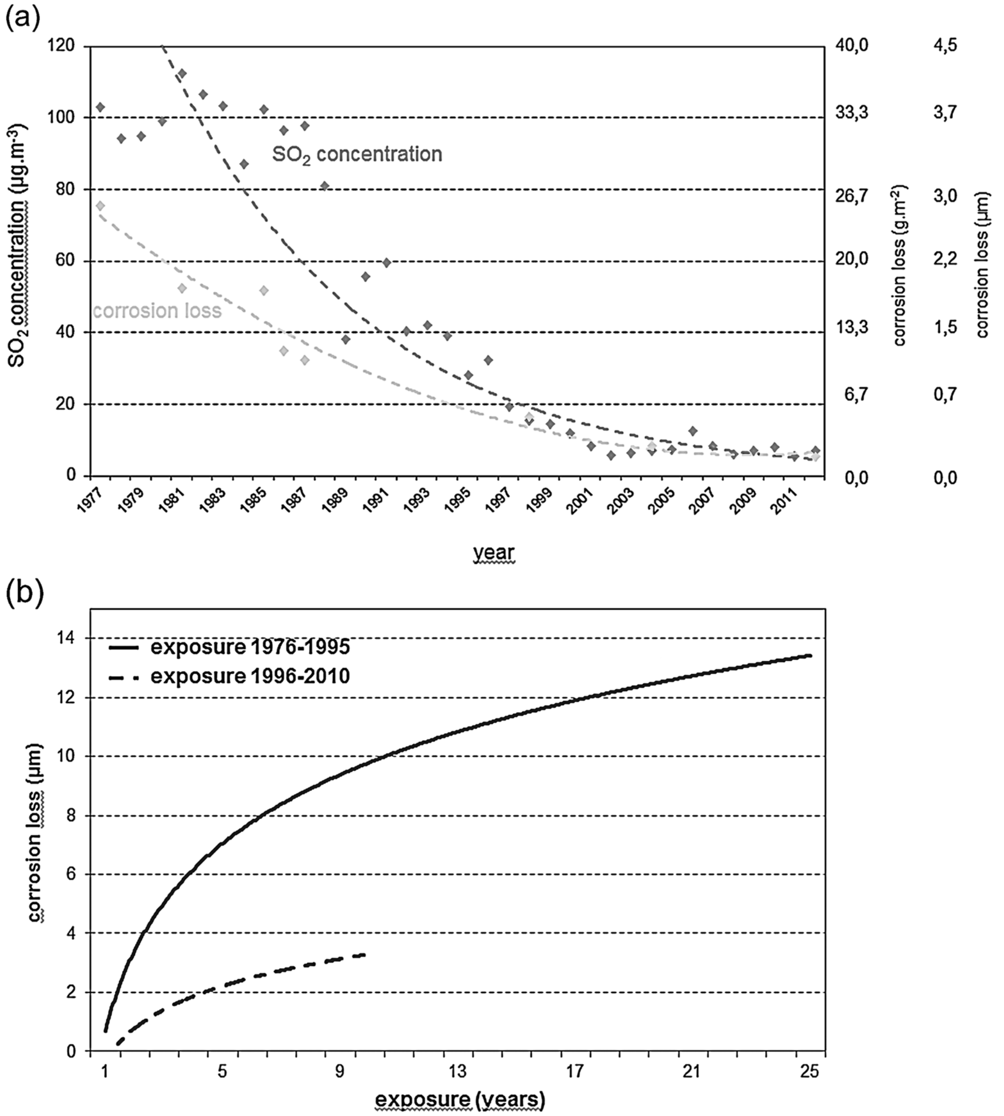

Figure 4. Corrosion mass loss of copper over various periods in Prague, Czech Republic; (a) repeated yearly exposure, (b) long-term exposure.

structural metals quickly reacts to decreasing SO_2. The surfaces exposed to a highly polluted environment showed a slowing in corrosion rate in case SO_2 pollution was lower in the atmosphere.

At the Czech test site the copper was exposed for 20 and 25 years, from 1981 to 2006. During this period the yearly value of SO_2 air pollution decreased from 145 μg.m^{-3} to 11 μg.m^{-3} in 2003, respectively 19 μg.m^{-3} in 2006, while the other environmental parameters were probably stable [10]. The corrosion mass loss fell in the newly exposed samples and the samples exposed to a highly polluted environment showed a slowing in corrosion rate in case SO_2 pollution had been reduced in the atmosphere – Figure 5. This is very important for predicting the service life of existing structures or objects exposed for centuries to such environmental conditions.

4 Case studies

Because corrosion is a process that also takes place in a clean environment, a certain corrosion rate must always be taken into consideration. This background corrosion rate depends on local climatic situations. In the Europe region, 1-year background corrosion losses were estimated at:

copper	3.0 g m^{-2}	0.30 μm
bronze	2.1 g m^{-2}	0.25 μm

This background corrosion mass loss for copper was not yet obtained at the majority of UN ECE ICP test sites (exposure period 2011/12).

The corrosivity of the atmosphere in the Prague centre where both objects are located was very high in the past due to industrial pollution and emissions from heating. The air SO_2 pollution in the Prague centre was 90 μg.m^{-3} in period 1970 - 90 and was about 15 μg.m^{-3} for the last 20 years [18]. During the 1970s and 1980s, when the air pollution reached its highest concentration, the corrosivity of the atmosphere in the Prague centre fell in category C5 according to EN ISO 9223.

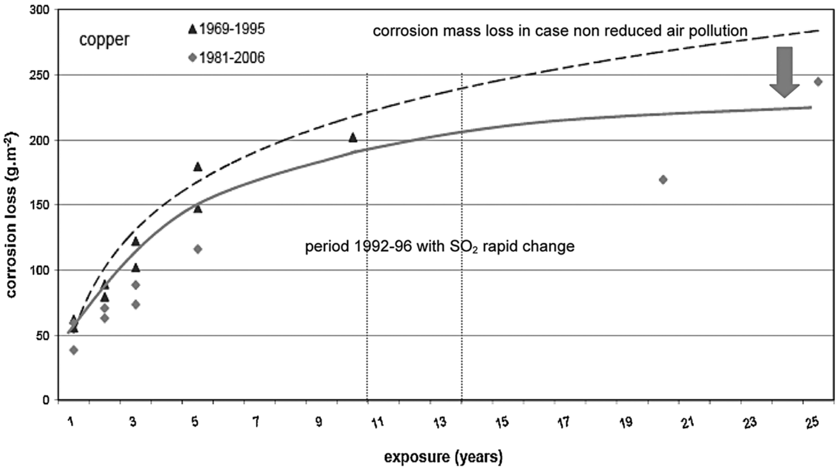

Figure 5. Changes in long-term corrosion behaviour of copper in atmosphere with changing corrosivity.

At that time the effect of NO_2 was not so important but in the contemporary multi-pollutant situation it is necessary to include its concentration in corrosion prediction models. NO_2 is soluble in water and reacts with water absorbed into surfaces to give nitric acid. Copper alloys are especially very sensitive to this type of pollution.

The climatic conditions are relatively steady during the period when pollution and the copper corrosion rate have been measured – there are records for temperature and precipitation since 1775. The difference in annual average temperature of 0.9 °C has no significant effect on the corrosion rate of copper alloys.

4.1 Copper roof of Queen Ann's Summer Palace

The long-term behaviour of copper corrosion was investigated on many cultural historical buildings in the Czech Republic [11]. One studied in detail is the copper roof of Queen Ann's Summer Palace, built in 1558–1564 (Figure 6). Some parts of the copper roof were replaced over the centuries (the first repair was recorded in 1688, large repairs were carried out in 1725-1726 followed by 6 other records) so now the roof is made up of sheets with different properties (including patina layers) after 300 to 100 or 30 years of exposure.

Figure 6. View of the west side of the Belveder roof in 2001 (before the first reconstruction).

The original thickness of the copper sheets was about 0.8 mm. The residual thickness after ca. 325 years varies from 0.35 to 0.50 mm in the most affected eastern ridge part. The residue thickness of other, less affected parts is about 0.6 mm. This represents a loss of ca. 200 μm and degradation rate ca. 0.6 $\mu m.a^{-1}$. This value should correspond to the steady corrosion rate in an atmosphere with corrosivity category C4 for copper according to EN ISO 9224. The highest loss of copper sheet thickness was estimated in the lower part on the west side of the roof, where long-term accumulation of water and deposits and mechanical stress and erosion by wind is expected. The application of best fitting prediction models shows the distribution of copper corrosion loss during this long-term exposure – Table 3. Both prediction models are relatively similar and correspond to the determined average long-term corrosion rate of 0.7 $\mu m.a^{-1}$. The time exponent coefficient applied in both models is too low ($b = 0.667$ or 0.835) for this real application of copper sheets. If this coefficient were 1, the total corrosion loss would be ca. 200 μm, which correspond to the determined value.

The variety of colours and compositions of the patina correspond to the shape arrangement of the roof. The thickness of the patina layer ranged from 7 to 142 μm with an average value of 44 μm. The dominant compound in the patina was brochantite ($Cu_4(SO_4)(OH)_6$), while other compounds such as cuprite and antlerite were found, too.

The limiting property for the serviceability of the roof was not corrosion (material) loss but the reduced mechanical properties. The strength R_m of historic sheet copper was only

Table 3. Estimated long-term copper corrosion loss according to various prediction models

period	estimated corrosion loss (μm)	
	ML_2	ML_3
1688-1950 (262 years)	16.1	19.9
1950-1995 (45 years)	10.2	12.6
1995-2013 (18 years)	8.3	4.7
total	34.6	37.2

Figure 7. Details of roof panels – cracks and penetrations (lower side of copper sheets).

156 MPa and the elongation only 10%. As a result of these conditions, there were cracks and perforations in the sheets with the minimum thickness (Figure 7).

4.2 Bronze statue of St. John of Nepomuk

There are 30 statues mounted to the balustrade of Charles Bridge in Prague. The statue of St. John of Nepomuk is the oldest on the bridge - the original is from 1683 (Figure 8). The original clay design was made by Austrian sculptor *Matthias Rauchmüller*, based upon a wood model by *Jan Brokoff*. The statue was then cast in bronze by *Volfgang Jeroným Heroldt* in Nuremberg.

In 1996 measuring of the bronze thickness was performed - the minimum value was 2.4 mm and in some areas it was ca. 5.0 mm depending on the design and shape of the statue (Figure 8). The critical residual thickness for bronze statues was estimated at 2.0 mm.

Small holes in the forehead and cap of the statue were recorded in the year 1989 (Figure 9). These defects occurred as a result of corrosion loss of the bronze material in these most exposed areas. From a photo taken in 1910 there is an indication that the cap was gilded and this layer protected the surface of bronze.

An analysis of corrosion products shows their typical urban composition (brochantite, cuprite, $(NH_4)_2Cu(SO_4)_2.6H_2O$), anglesite, $PbSO_4$), pollution (quartz) and residua from surface treatment (graphite).

The application of best fitting prediction models shows the distribution of bronze corrosion loss during this long-term exposure – Table 4. Both prediction models are very different. On the actual object the mass of bronze affects the duration of

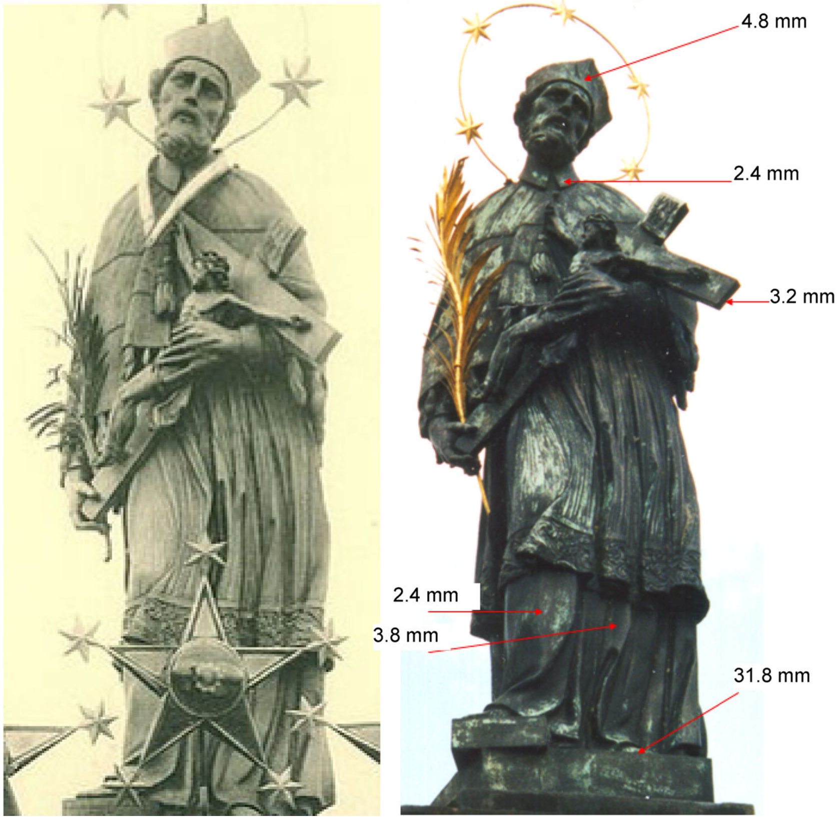

Figure 8. St. John of Nepomuk statue on Charles bridge (1910 and 1998) with bronze thickness measuring areas.

Figure 9. Detail of bronze surface with open holes.

Table 4. Estimated long-term bronze corrosion loss according to various prediction models

period	estimated corrosion loss (μm)	
	ML_2	ML_3
1683-1950 (267 years)	49.3	14.1
1950-1995 (45 years)	39.3	8.8
1995-2013 (18 years)	9.9	3.3
total	98.5	26.4

wetness of the surface and increases corrosion stress. Its location on the bridge means it is extremely affected by mist and wetness.

5 Conclusion

Many copper and bronze cultural heritage objects in Prague were inspected. It is necessary to differentiate between corrosion damage on sculptures and on roofs and cladding. Corrosion-mechanical manifestations on roofs and cladding lead to a reduction in the lifetime of these objects, while corrosion characteristics on sculptures are mostly aesthetic with the exception of corrosion of the inner skeleton or the joints. Uneven corrosion along grains was observed in a limited number of cases on horizontal and less inclined surfaces of statues exposed to highly polluted environments. Bimetallic corrosion occurs in places where a steel inner construction is in contact with a copper alloy surface.

Different prediction models of atmospheric corrosion rate may also be used for historic materials of cultural heritage. All performed prediction models were derived from a relatively limited database, especially with respect to the exposure period.

Regardless of the applied model, the 50-year period with high air pollution (SO_2, pH, etc.) from 1950-1995 caused practically the same corrosion loss of copper alloys as the previous 250 years of exposure for these historic long-term exposed cultural objects in Prague. The situation was very similar in other European urban localities. Atmospheric tests performed in contemporary atmospheres cannot represent the long-term exposure of copper alloy objects and short (1-year) corrosion data may be misleading [12].

While, there may be other factors that affect the durability of these metallic materials after centuries' exposure, it is still important to understand the basic corrosion mechanisms for outdoor copper and its alloys in predicting long-term maintenance including costs.

6 References

[1] J. Tidblad, V. Kucera, A.A. Mikhailov, J. Henriksen, K. Kreislova, T. Yates, B. SInger, in: *ASTM ATP 1421 Outdoor Atmospheric Corrosion*, H.E. Townsend, (Ed.), ASTM International, West Conshohocken, PA, **2002**, pp. 73–87.

[2] D. Knotkova, V. Kucera, S.W. Dean, P. Boschek, in: *ASTM ATP 1421 Outdoor Atmospheric Corrosion*, H.E. Townsend, (Ed.), ASTM International, West Conshohocken, PA, **2002**, pp. 109- 126.

[3] D. Knotkova, P. Boschek, K. Kreislova in: *ASTM STP 1239 Atmospheric corrosion*, W.W. Kirk and H.H. Lawson (Eds.), American Society for Testing and Materials, Philadelphia, **1995**, p. 38.

[4] S.W. Dean, D.B. Reiser, *CORROSION 98, NACE International*, Houston, TX, **1998**, 340.

[5] M. Morcillo, Atmospheric CorrosioninIbero-America: The Micat Project, ASTM STP 1239 *Atmospheric corrosion*, W.W. Kirk and H.H. Lawson (Eds.), Philadelphia, **1995**, pp. 257–275.

[6] T.E. Graedel, K. Nassau, J.P. Franey, *Corr. Sci.* **1987**, *27*, 639.

[7] *EN ISO* 9223: **2012** Corrosion of metals and alloys—Corrosivity of atmospheres— Classification, determination and estimation.

[8] *EN ISO* 9224: **2012** Corrosion of metals and alloys—Corrosivity of atmospheres—Guiding values for the corrosivity categories.

[9] B. Stöckle, A. Krätschmer, M. Mach, R. Snethlage, *Report No 23 Corrosion attack on copper and cast bronze. Evaluation after 8 years of exposure, UNECE International co-operative programme on effects on materials, including historic and cultural monuments*. Bavarian State Conservation Office, Münich, Germany, **1998**.

[10] *UN ECE ICP Report No 72*, Results of corrosion and soiling from the 2011-2012 exposure programme for trend analysis, Swerea, KIMAB, Stockholm **2013**.

[11] D. Knotková, K. Kreislová, *Atmospheric corrosion and conservation of copper and bronze*, A. Moncmanová (Eds.), WIT Press Publ. Advances in Architecture, Southampton **2007**, 107–142.

[12] B. De Filippo, D. Ferro, R. Natalini, in: *Proceedings of EUROCORR 2013*, Estoril, Portugal.**2013**, *1–5* 9.

(Received: October 31, 2014) W8112
(Accepted: May 11, 2015)